第 32 卷第 7 期
2016 年 7 月

无 机 化 学 学 报
CHINESE JOURNAL OF INORGANIC CHEMISTRY

Vol.32 No.7
1231-1238

柔性配体构筑的三个构象多样的镧系羧酸配位聚合物：合成，结构和荧光性质

崔培培*,[1] 崔论峰[2] 符爱云[1]

([1]德州学院生命科学学院，德州 253023)

([2]潍坊市朱里中学，潍坊 261111)

摘要：利用 2,2′-(1,4-亚苯基)二(亚苯基)二(硫基)苯二羧酸(H_2L^1)和 2,2′-(2,3,5,6-四甲基-1,4-亚苯基)二(亚甲基)二(硫基)苯二甲酸(H_2L^2)2 个柔性二羧酸分别与镧系金属盐反应，通过溶剂热方法合成了 3 个配位聚合物：$\{[(NH_2(CH_3)_2][Nd(L^1)_2(DMF)]\cdot 2DMF\}_n$(**1**)和 $\{[Ln(L^2)_{1.5}(H_2O)(DMF)_2]\cdot 2DMF\}_n$[Ln=Ce(**2**)，Pr(**3**)]。利用元素分析、红外、粉末 X 射线衍射、热重分析等对配合物进行了表征。X 射线单晶衍射分析表明：3 个配合物均为二维的层状结构，并且 2 个配体在配合物中表现出不同的构象。$(L^1)^{2-}$在配合物 **1** 中表现出顺式和反式 **2** 种构象，$(L^2)^{2-}$在配合物 **2** 和 **3** 中仅表现出反式构象。此外，对配合物的热稳定性和荧光性质也进行了研究。

关键词：配位聚合物；柔性配体；构象；荧光性质

中图分类号：O614.33+2；O614.33+4；O614.33+5　　**文献标识码**：A　　**文章编号**：1001-4861(2016)07-1231-08

DOI：10.11862/CJIC.2016.155

Three Lanthanide-Carboxylate Coordination Polymers with Conformation Variation Based on Flexible Ligands: Syntheses, Structures and Photoluminescence Properties

CUI Pei-Pei*,[1] CUI Lun-Feng[2] FU Ai-Yun[1]

([1]*College of Life Science, Dezhou University, Dezhou, Shandong* 253023, *China*)

([2]*Zhuli Middle School, Weifang, Shandong* 261111, *China*)

Abstract: Reactions of flexible dicarboxylate ligands 2,2-(1,4-phenylenebis (methylene))bis(sulfanediyl)dibenzoic acid (H_2L^1) and 2,2-(2,3,5,6-tetramethyl-1,4-phenylene)bis(methylene)bis(sulfanediyl) dibenzoic acid (H_2L^2) with lanthanide metal salts under solvothermal conditions give rise to three lanthanide-organic coordination polymers (CPs), namely, $\{[(NH_2(CH_3)_2][Nd(L^1)_2(DMF)]\cdot 2DMF\}_n$(**1**) and $\{[Ln(L^2)_{1.5}(H_2O)(DMF)_2]\cdot 2DMF\}_n$ [Ln=Ce(**2**), Pr(**3**)] (DMF=*N*,*N*-dimethylformamide). All of the complexes have been structurally characterized by single-crystal X-ray diffraction analyses and characterized by elemental analysis, infrared spectra (IR), powder X-ray diffraction (PXRD), and thermogravimetric analysis (TGA). All the complexes have two-dimensional (2D) layer structures, which can be simplified as (4,4) net. The ligands display different conformation. $(L^1)^{2-}$ in complex **1** exhibits two kinds of conformations: *syn*- and *anti*-conformation, while $(L^2)^{2-}$ in complexes **2** and **3** exhibits *anti*-conformation. Furthermore, the thermal stabilities and photoluminescence properties of the complexes were investigated. CCDC: 1482586, **1**; 1482588, **2**; 1482587, **3**.

Keywords: coordination polymers; flexible ligand; conformation; photoluminescence property

收稿日期：2015-12-25。收修改稿日期：2016-05-10。

国家自然科学基金(No.21171031)资助项目。

*通信联系人。E-mail：1cuipeipei1@163.com

0 Introduction

The synthesis and characterization of coordination polymers (CPs) is one of the most rapidly developing areas of chemical science, not only due to their interesting structures and topologically diverse, but also because of their potential applications, such as photoluminescence property, gas storage, catalysis [1-5]. According to the composition of CPs, the certain features of ligands are crucial to construct CPs, such as flexibility, appropriate functional groups and versatile binding modes [6-10]. In general, the conformation of the ligands can determine the final structure of CPs. Compared with the single conformation of the rigid ligands, many kinds of conformation exist for the flexible ligands. Thus, it is difficult to predict the final structures for flexible ligands[11-16].

As we all know, the research in the construction of CPs is mainly in the rigid ligands and the systemic research of the flexible ligands is considerably rare. Although the difficulty of structural prediction exists, the design and synthesis of CPs employing flexible ligands still have attracted lots of researchers interests [17-20]. In order to explore the relationships between the conformation of the ligands and the final structure, more and more attention was paid. In the past few years, our group have designed and synthesized a series of flexible carboxylate ligands to construct CPs [21-26]. Based on our previous work, we designed and synthesized two flexible discarboxylate ligands, 2,2-(1,4-phenylenebis (methylene))bis (sulfanediyl)dibenzoic acid (H_2L^1) and 2,2-(2,3,5,6-tetramethyl-1,4-phenylene)bis (methylene)bis (sulfanediyl) dibenzoic acid (H_2L^2) (Scheme 1). Three CPs, $\{[(NH_2(CH_3)_2][Nd(L^1)_2(DMF)]\cdot 2DMF\}_n$ (**1**) and $\{[Ln(L^2)_{1.5}(H_2O)(DMF)_2]\cdot 2DMF\}_n$ [Ln =Ce (**2**), Pr (**3**)], have been synthesized. Although the conformation of the ligands are different in complexes **1** ~**3**, all the complexes have two-dimensional (2D) layer structures with (4,4) net. Among them, $(L^1)^{2-}$ exhibits two kind conformation: syn- and anti-conformation in complex **1**, while $(L^2)^{2-}$ exhibits only one conformation: anti-conformation in complexes **2** and **3**. In addition, the thermal stability and photoluminescence property of the complexes were investigated.

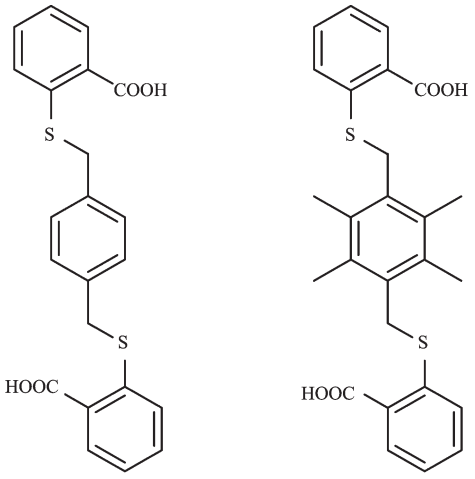

H_2L^1 H_2L^2

Scheme 1 The flexible carboxylate ligands used in this work

1 Experimental

1.1 Materials and methods

All commercially available chemicals and solvents are of reagent grade and were used as received without further purification. The ligands H_2L^1 and H_2L^2 were synthesized according to the procedure reported in the literature [27-28]. Elemental analysis for C, H, and N was

performed on a Perkin-Elmer 240 C Elemental Analyzer. FTIR spectra was recorded in the range of 400 ~4 000 cm^{-1} on a Bruker Vector 22 FTIR spectrophotometer using KBr pellets. Thermogravimetric analysis (TGA) was performed on a simultaneous SDT 2960 thermal analyzer under nitrogen with a heating rate of 10 ℃·min^{-1}. Powder X-ray diffraction (PXRD) patterns were obtained on a Bruker D8 Advance diffractometer using Cu $K\alpha$ radiation source (λ = 0.154 18 nm) at 293 K, in which the X-ray tube was operated at 40 kV and 40 mA. Photoluminescence properties for the powdered solid samples were measured on an Aminco Bowman Series **2** spectrofluorometer with a xenon arc lamp as the light source.

1.2 Synthesis of complexes 1~3

1.2.1 Synthesis of complex **1**

H_2L^1 (4.1 mg, 0.01 mmol), 1,3-di(pyridine-4-yl) propane (1.5 mg, 0.008 mmol) and $Nd(NO_3)_3·6H_2O$ (7.8 mg, 0.018 mmol) were dissolved in 1.5 mL of DMF/EtOH/H_2O (5∶2∶1,*V*/*V*) in a glass tube. The glass tube was sealed and left at 90 ℃ for 3 days. The resulting purple block crystals were collected in 50% yield based on H_2L^1. Elemental analysis Calcd. for $C_{55}H_{61}N_4O_{11}S_4Nd$ (%): C 53.86, H 5.01, N 4.57; Found (%): C 53.67, H 4.83, N 4.36 . Selected IR peaks (cm^{-1}, Fig.S5a): 3 448 (s), 1 672 (s), 1 623 (s), 1 538 (s), 1 394 (s), 1 014 (m), 859 (w), 786 (m), 673 (w).

1.2.2 Synthesis of complex **2**

The synthesis of **2** is similar to **1** except that H_2L^2 (4.7 mg, 0.01 mmol) and $Ce(NO_3)_3·6H_2O$ (7.8 mg, 0.018 mmol) were used instead of H_2L^1 and $Nd(NO_3)_3·6H_2O$. The resulting colorless block crystals were collected in 60% yield based on H_2L^2. Elemental analysis Calcd. for $C_{51}H_{66}O_{11}N_4S_3Ce$ (%): C 53.39, H 5.80, N 4.88; Found (%): C 53.67, H 5.83, N 4.46. Selected IR peaks (cm^{-1}, Fig. S5b): 3 378 (s), 1 644 (s), 1 597 (s), 1 549 (s), 1 440 (w), 1 388 (s), 1 320 (w), 1 183 (w), 1 055(w), 814(m), 782(w).

1.2.3 Synthesis of complex **3**

Complex **3** was obtained by the same procedure used for the preparation of **2** except that $Ce(NO_3)_3·6H_2O$ was replaced by $Pr(NO_3)_3·6H_2O$. After cooling to room temperature, the resulting green block crystals were collected in 55% yield based on H_2L^2. Elemental analysis Calcd. for $C_{51}H_{66}O_{11}N_4S_3Pr$ (%): C 53.35, H 5.79, N 4.88; Found (%): C 53.47, H 5.83, N 4.46 . Selected IR peaks (cm^{-1}, Fig. S5c): 3 399 (s), 1 658 (s), 1 603 (s), 1 535 (s), 1 394 (s), 1 097 (w), 859 (w), 787 (m), 703 (w).

1.3 Crystallographic data collection and refinement

Diffraction data for **1~3** were collected on a Bruker Smart Apex Ⅱ CCD with graphite monochromated Mo $K\alpha$ radiation source (λ =0.071 073 nm) in φ-ω scan mode. The diffraction data were integrated by using the SAINT program[29], which was also used for the intensity corrections for the Lorentz and polarization effects. Semi-empirical absorption corrections were applied using SADABS program[30]. All the structures were solved by direct methods using SHELXS-97[31] and the non-hydrogen atoms were refined on F^2 by full-matrix least-squares procedures with SHELXL-97 for **1**[32] and SHELXL-2014 for **2** and **3**[33]. For **2** and **3**, the SQUEEZE subroutine of the PLATON software suite was applied to remove the scattering from the highly disordered solvent molecules[34]. The final formulas were calculated from the SQUEEZE results, TGA and elemental analysis. Hydrogen atoms except those of water molecules were generated geometrically and refined isotropically using the riding model. The hydrogen atoms of coordinated water molecules were found directly. The details of the crystal parameters, data collection and refinements for **1~3** are summarized in Table 1. Selected bond lengths and angles for **1~3** are listed in Table S1. The parameters of hydrogen bonds for **1** are listed in Table S2.

CCDC: 1482586, **1**; 1482588, **2**; 1482587, **3**.

Table 1　Crystal data and structure refinements for complexes 1~3

Complex	**1**	**2**	3
Formula	$C_{55}H_{61}N_4O_{11}S_4Nd$	$C_{51}H_{66}N_4O_{11}S_3Ce$	$C_{51}H_{66}N_4O_{11}S_3Pr$
Formula weight	1 226.56	1 147.37	1 148.16

Continued Table 1

Crystal system	Triclinic	Triclinic	Triclinic
Space group	$P\bar{1}$	$P\bar{1}$	$P\bar{1}$
a / nm	0.825 27(6)	1.266 8(2)	1.265 59(7)
b / nm	1.544 81(11)	1.458 5(3)	1.456 99(8)
c / nm	2.285 05(16)	1.732 3(3)	1.730 71(9)
α / (°)	96.381 0(10)	113.754(2)	113.796 0(10)
β / (°)	96.700 0(10)	109.044(2)	109.001 0(10)
γ / (°)	98.706 0(10)	90.263(2)	90.365 0(10)
V / nm^3	2.835 2(4)	2.734 7(9)	2.725 7(3)
Z	2	2	2
D_c / (g·cm^{-3})	1.437	1.393	1.399
μ / mm^{-1}	1.124	1.006	1.068
F(000)	1 262	1 188	1 190
Unique reflections	9 898	9 975	10 265
Obsd. reflections [$I>2\sigma(I)$]	14 208	12 289	13 092
Parameters	672	527	527
GOF	1.082	1.047	1.129
Final R indices [$I>2\sigma(I)$][a,b]	R_1=0.046 2,	R_1=0.038 1,	R_1=0.042 9,
	wR_2=0.275	wR_2=0.097 1	wR_2=0.115 0
R indices (all data)	R_1=0.058 4,	R_1=0.049 1,	R_1=0.057 4,
	wR_2=0.146 2	wR_2=0.101 7	wR_2=0.121 3
Largest diff. peak and hole / (e·nm^{-3})	828 and −1 239	716 and −1 504	889 and −1 965

[a] $R_1=\Sigma||F_o|-|F_c||/\Sigma|F_o|$, [b] $wR_2=[\Sigma w(F_o^2-F_c^2)^2]/\Sigma w(F_o^2)^2]^{1/2}$

2 Results and discussion

2.1 Crystal structures of 1~3

2.1.1 Crystal structure of **1**

Single crystal X-ray structural analysis reveals that complex **1** crystallizes in the triclinic $P\bar{1}$ space group. As shown in Fig.1a, the Nd(Ⅲ) is nine-coordinated by eight carboxylate oxygen atoms from four $(L^1)^{2-}$ ligands and one oxygen atom from coordinated DMF molecule. The asymmetric unit of **1** contains one molecule of $[(NH_2(CH_3)_2][Nd(L^1)_2(DMF)]\cdot 2DMF$. As observed previously, the dimethyl ammonium cation is generated by in situ decomposition of DMF under the solvothermal reaction conditions [35-36]. All the H_2L^1 ligands are deprotonated during the reaction. As shown in Fig.1b, although all carboxylate groups of the ligands adopt chelating mode, there are two conformation for $(L^1)^{2-}$ ligand in **1**: the *syn*-conformation (mode Ⅰ) and the *anti*-conformation (mode Ⅱ). On one hand, in the structure of complex **1** each *syn*-conformational $(L^1)^{2-}$ ligands links two Nd(Ⅲ) ions to generate a 1D chain along *a* axis (Fig.S1a). On the other hand, along *b* axis, each *anti*-conformational $(L^1)^{2-}$ ligand links two Nd(Ⅲ) ions to generate a 1D chain, too (Fig.S1b). Two kinds of chains connect together with Nd(Ⅲ) ions extending along *ab* plane to form a 2D layer and the layer can be simplified as (4,4) net (Fig.1c). More interesting, two adjacent chains with the *anti*-conformational $(L^1)^{2-}$ ligands were linked by the *syn*-conformational $(L^1)^{2-}$ ligands to form a 1D incomplete closed channel (Fig.1d and 1e). In addition, there are hydrogen bonds to stabilize the structure (Table S2).

2.1.2 Crystal structure of **2**

When four $-CH_3$ were added in the central benzene ring of H_2L^1, H_2L^2 was obtained. By the similar procedure used for the preparation of complex **1**, complexes **2** and **3** were obtained. Single crystal X-

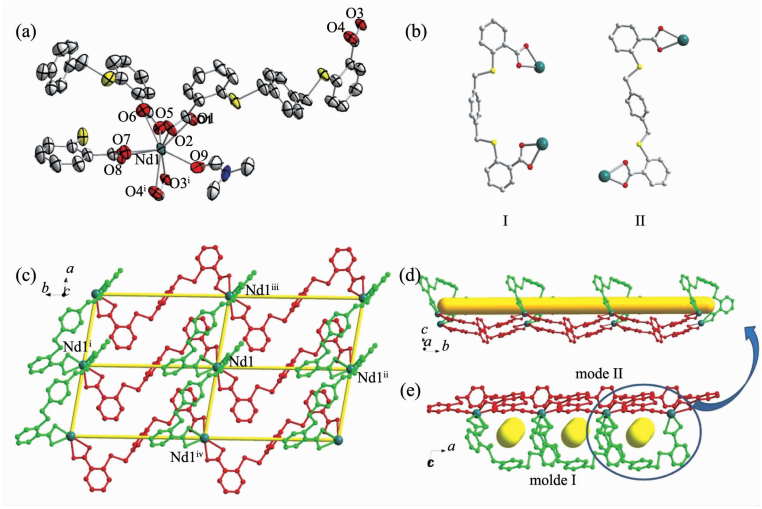

Symmetry codes: [i] $x, y+1, z$; [ii] $x, y-1, z$; [iii] $x+1, y, z$; [iv] $x-1, y, z$

Fig.1　(a) The coordination environment of Nd(Ⅲ) ion in complex **1** with 50% thermal ellipsoid probability; (b) Two conformation and coordination modes in complex **1**; (c) Schematic representation from the 2D layer to (4,4) net; (d) The 1D channel in complex **1**; (e) The 2D layer containing 1D channels viewed along *b* axis

ray structural analysis reveals that complexes **2** and **3** are isostructural, thence the structure of complex **2** is discussed as an example. Complex **2** crystallizes in the triclinic $P\bar{1}$ space group. The asymmetric unit of **2** consists of one Ce(Ⅲ) ion, one and half $(L^2)^{2-}$ ligands, one coordinated water molecule, two coordinated DMF molecules and two uncoordinated DMF molecules. The Ce(Ⅲ) ion is coordinated by nine oxygen atoms, in which six oxygen atoms from four $(L^2)^{2-}$ ligands and three from coordinated solvents (Fig.2a). Two adjacent Ce(Ⅲ) ions linked together by two carboxylate groups with bridging chelate mode to form a binuclear

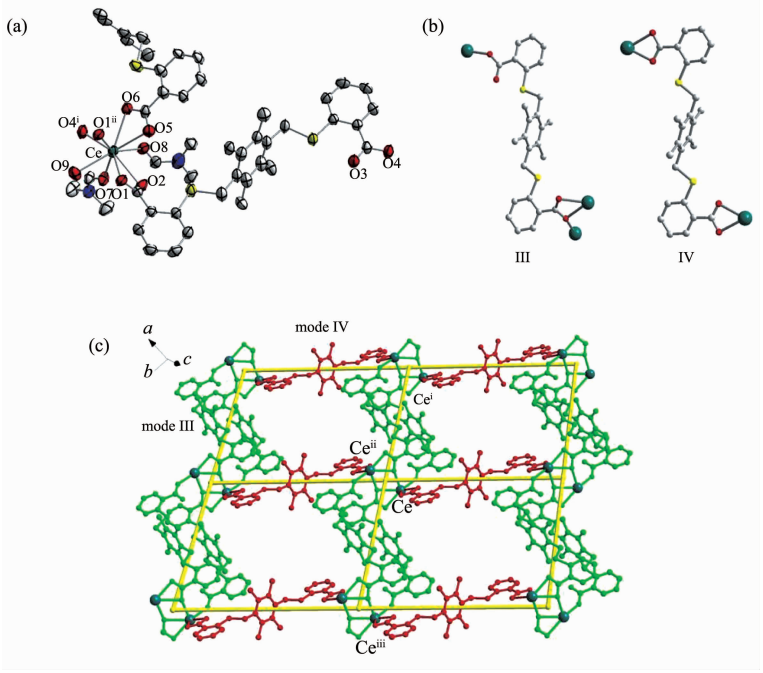

Symmetry codes: [i] $x, y-1, z-1$; [ii] $-x+2, -y, -z$; [iii] $x, y+1, z+1$

Fig.2　(a) Coordination environment of Ce(Ⅲ) ion in **2** with 50% thermal ellipsoid probability; (b) Two coordination modes in **2** with *anti*-conformation; (c) 2D layer of complex **2**

secondary building unit (SBU), which is engaged by six carboxylate groups (Fig.S3). All carboxyl groups are deprotonated and all $(L^2)^{2-}$ ligands adopt the anti-conformation. However, the $(L^2)^{2-}$ ligands have two different coordination modes (Fig.2b). The first connects three Ce(Ⅲ) ions using two carboxylate groups with monodentate and bridging chelate mode, respectively (mode Ⅲ). The second connects two Ce(Ⅲ) ions using two carboxylate groups with chelating mode (mode Ⅳ). The $(L^2)^{2-}$ ligands with mode Ⅲ connect Ce(Ⅲ) ions to form a 1D double chain, while the $(L^2)^{2-}$ ligands with mode Ⅳ act as linkers to join the Ce(Ⅲ) ions to generate a 1D single chain (Fig.S4). Such two type chains are joined together to provide the 2D layer structure in complex **2** (Fig.2c). If the ligands can be considered as a single linker and the binuclear SBU as a 4-connected node, then the 2D layer possesses a (4,4) net, which is same to complex **1**.

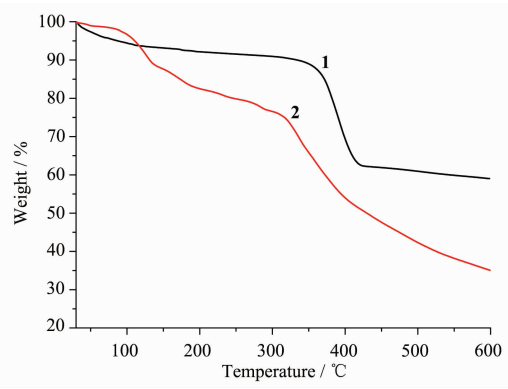

Fig.3 TGA curves of **1** and **2**

2.2 Synthesis of the complexes and comparison of the structures

Three lanthanide-organic frameworks were synthesized and characterized based on the flexible discarboxylate ligands 2,2-(1,4-phenylenebis (methylene))bis (sulfanediyl)dibenzoic acid (H_2L^1) and 2, 2-(2,3,5,6-tetramethyl-1,4-phenylene)bis (methylene) bis(sulfanediyl) dibenzoic acid (H_2L^2). They are all 2D layer structures. The deprotonation of the carboxylic acids to the corresponding carboxylate ligands was confirmed by crystal structural analyses as described above as well as by IR spectra, because no obvious bands between 1 680 and 1 760 cm^{-1} originated from the carboxylic group (-COOH) were found (Fig.S5). The coordination mode and conformation of the $(L^1)^{2-}$ and $(L^2)^{2-}$ ligands have similarities and differences, which may be attributed to the difference of the ligand geometry. In the $(L^1)^{2-}$ and $(L^2)^{2-}$ ligands, the two 2-mercaptobenzoic acid groups are located in the 1,4-positions of the central benzene rings. So the two carboxylate groups are separated the farthest and the two flexible arms of one ligand are difficult to chelate one metal center. Therefore, all ligands are coordinated with two metal centers in **1**~**3**. More interesting, the $(L^1)^{2-}$ ligand adopts an *anti*-conformation in the previous report [37], while in **1** it has two conformation, *syn*- and *anti*-conformation. For the $(L^2)^{2-}$ ligand, the *syn*- and *anti*-conformation have been reported[20,22,37]. In **2** and **3**, it has only one conformation that is *anti*-conformation (Fig.2b). In addition, although 1,3-di(pyridin-4-yl)propane does not exist in the final structures, it should be pointed out that it may play important role in the formation of **1**~**3**, due to that no crystals were obtained without addition of 1,3-di (pyridin-4-yl)propane in the synthetic reactions.

2.3 Powder X-ray diffraction and thermogravimetric analyses

The purity and stability of coordination polymers are important for CPs practical application, so the powder X-ray diffraction (PXRD) and thermogravimetric analysis (TGA) of complexes **1** and **2** were measured. Due to complexes **2** and **3** are isostructural, we choose complex **2** as an example to discuss. The phase purity of the bulky sample was checked by PXRD. The result shows that the measured PXRD pattern of the experimental sample closely matches the simulated one, indicating the pure phase of the product (Fig.S6).

The thermal stability of **1** and **2** was examined by TGA in the N_2 atmosphere from 30 to 600 ℃ (Fig.3). The results indicate that complex **1** shows a weight loss of 11.2% before 300℃, which correspond to the release of two free DMF molecules (Calcd. 11.9%), and the further weight loss was observed at about 350℃, owing to the collapse of the frameworks of **1**. For complex **2**, the first weight loss of 12.1% from 30 to 130 ℃ is in accordance with the loss of free DMF

molecules (Calcd. 12.7%). The second weight loss of 13.9% from 130 to 310 ℃ is in accordance with the loss of coordinated DMF and H_2O molecules (Calcd. 14.2%). After 310 ℃, complex **2** starts to decompose.

2.4 Photoluminescence property

Photoluminescence property of CPs has attracted much attention due to the possible emission and application in chemical sensors, photochemistry and electroluminescent displays and so on[38-41]. Thence, the photoluminescence properties of **1~3** in the solid state were investigated at room temperature (Fig.4). The photoluminescence property of H_2L^2 ligand has been reported and H_2L^2 ligand exhibits emission at 398 nm upon excitation at 320 nm[22]. Here, H_2L^1 ligand was investigated in order to comparison and the maximum emission band is at *ca.* 372 nm excited at 320 nm, which is probably attributed to the $\pi\rightarrow\pi^*$ electronic transition. Complex **1** shows the maximum emission bands at *ca.* 370 nm upon excitation at 320 nm. The emission can be assigned to an intraligand $\pi\rightarrow\pi^*$ electronic transition, because it is similar to the emission of free H_2L^1 ligand. For complexes **2** and **3**, the maximum emission bands are at 393 nm for **2** and 387 nm for **3** (λ_{ex}=320 nm). Compared to the free ligand H_2L^2, the emission maxima of **2** and **3** are bule-shift, which may be attributed to the coordination of the ligand to the metal center[42-44].

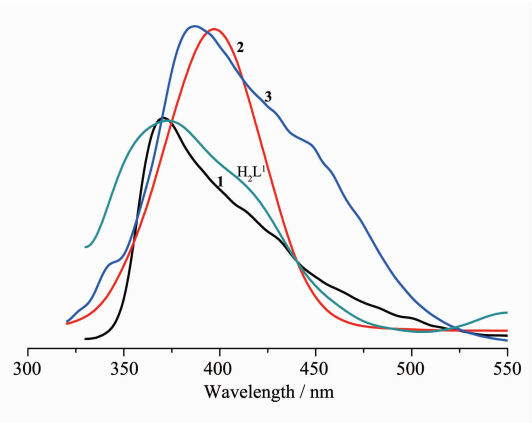

Fig.4 Emission spectra of **1~3** as well as free H_2L^1 ligand in the solid state at room temperature

3 Conclusions

In summary, three lanthanide-organic CPs based on the flexible dicarboxylate ligands H_2L^1 and H_2L^2 were synthesized and characterized. The structures of them are 2D layers and the layers can be simplified as (4,4) net. For the ligands, they show different conformation and coordination modes. The results illustrate that the positions of the functional substituent on the central ring and the conformation of the ligands play important roles in governing the structures of CPs. Furthermore, the thermal stability and photoluminescence property of the complexes were investigated.

Supporting information is available at http://www.wjhxxb.cn

References:

[1] Timmons A J, Symes M D. *Chem. Soc. Rev*., **2015**,**44**:6708-6722

[2] Li M, Li D, OKeeffe M, et al. *Chem. Rev*., **2014**,**114**:1343-1370

[3] Zhang W, Xiong R. *G. Chem. Rev*., **2012**,**112**:1163-1195

[4] Zhang J P, Zhang Y B, Lin J B, et al. *Chem. Rev*., **2012**, **112**:1001-1033

[5] Xuan W, Zhu C, Liu Y, et al. *Chem Soc Rev*., **2012**,**41**: 1677-1695

[6] Cook T R, Zheng Y R, Stang P J. Chem. Rev., 2013,113: 734-777

[7] O′Keeffe M, Yaghi O M. *Chem. Rev*., **2012**,**112**:675-702

[8] Eddaoudi M, Kim J, Rosi N, et al. *Science*, **2002**,**295**:469-472

[9] Wang C, Zhang T, Lin W. *Chem. Rev*., **2012**,**112**:1084-1104

[10]Wong-Foy A G, Matzger A J, Yaghi O M. *J. Am. Chem. Soc*., **2006**,**128**:3494-3495

[11]Zhang, Z H, Song Y, Okamura T, et al. *Inorg. Chem*., **2006**, **45**:2896-2902

[12]Wu H, Liu H Y, Yang J, et al. *Chem. Commun*., **2011**,**47**: 1818-1820

[13]Sengupta S, Ganguly S, Goswami A, et al. *CrystEngComm*, **2012**,**14**:7428-7437

[14]Yang Y, Du P, Liu Y Y, et al. *Cryst. Growth Des*., **2013**,**13**: 4781-4795

[15]Liu L L, Yu C X, Ma F J, et al. *Dalton Trans*., **2015**,**44**: 1636-1645

[16]Bhardwaj V K. *Dalton Trans*., **2015**,**44**:8801-8804

[17]Evangelisti F, Guttinger R, Moré R, et al. *J. Am. Chem. Soc*., **2013**,**135**:18734-18737

[18]Liu H Y, Ma J F, Liu Y Y, et al. *CrystEngComm*, **2013**,**15**:

2699-2708

[19]Kong L Y, Zhang Z H, Zhu H F. *Angew. Chem. Int. Ed.*, **2005**,**44**:4352-4355

[20]Dai F N, Sun D, Sun D F. *Cryst. Growth Des*., **2011**,**11**: 5670-5675

[21]Cui P P, Wu J L, Zhao X L, et al. *Cryst Growth Des.*, **2011**,**11**:5182-5187

[22]Cui P P, Dou J M, Sun D, et al. *CrystEngComm*, **2011**,**13**: 6968-6971

[23]Dai F N, He H Y, Xie A P, et al. *CrystEngComm*, **2009**,**11**: 47-49

[24]Zhao X L, He H Y, Hu T P, et al. *Inorg. Chem*., **2009**,**48**: 8057-8059

[25]Dai F N, He H Y, Gao D L, et al. *CrystEngComm*, **2009**,**11**: 2516-2522

[26]Dai F N, Dou J M, He H Y, et al. *Inorg. Chem.*, **2010**,**49**: 4117-4124

[27]Yang C, Wong W T. Chem. Lett., **2004**,**33**:856-857

[28]Yang C, Wong W T, Chen X M, et al. *Sci. Chin. B*, **2003**,**46**:558-566

[29]*SAINT, Program for Data Extraction and Reduction*, Bruker AXS, Inc., Madison, WI, **2001**.

[30]Sheldrick G M. SADABS, University of Göttingen, Göttingen, Germany, **2003**.

[31]Sheldrick G M. *SHELXS*-97, *Program for Crystal Structure Solution*, University of Göttingen, Göttingen, Germany, **1997**.

[32]Sheldrick G M. *SHELXL*-97, *Program for Crystal Structure Refinement*, University of Göttingen, Göttingen, Germany, **1997**.

[33]Sheldrick G M. *SHELXL*-2014, *Program for Crystal Structure Refinement*, University of Göttingen, Göttingen, Germany, **2014**.

[34]Spek A L. *PLATON, A Multipurpose Crystallographic Tool*, Utrecht University, The Netherlands, **2013**.

[35]Hendon C H, Tiana D, Fontecave M, et al. *J. Am. Chem. Soc.*, **2013**,**135**:10942-10945

[36]Li P Z, Wang X J, Li Y, et al. *Microporous Mesoporous Mater.*, **2013**,**176**:194-198

[37]Dai F N, Gong S W, Cui P P, et al. *New J. Chem.*, **2010**,**34**: 2496-2501.

[38]Cui P P, Zhang X D, Zhao Y, et al. *Microporous Mesoporous Mater*., **2015**,**208**:188-195

[39]Cui P P, Zhao Y, Zhang X D, et al. *Dyes Pigm*., **2016**,**124**: 241-248

[40]Lin Z J, Xu B, Liu T F, et al. *Eur. J. Inorg. Chem.*, **2010**: 3842-3849

[41]Cui Y J, Yue Y F, Qian G D, et al. *Chem. Rev*., **2012**,**112**: 1126-1162

[42]Sun D F, Ma S Q, Ke Y X, et al. *Chem. Commun*, **2005**,**21**: 2663-2665

[43]Zhan C, Zou C, Kong G Q, et al. *Cryst. Growth Des*., **2013**,**13**:1429-1437

[44]Zhao J, Wang X L, Shi X, et al. *Inorg. Chem*., **2011**,**50**: 3198-3205